43rd IEEE Conference on Decision and Control
December 14-17, 2004
Atlantis, Paradise Island, Bahamas

Approaches to Vision-Based Formation Control

Eric N. Johnson, Anthony J. Calise, Ramachandra Sattigeri, Yoko Watanabe and Venkatesh Madyastha

Abstract—**This paper implements several methods for performing vision-based formation flight control of multiple aircraft in the presence of obstacles. No information is communicated between aircraft, and only passive 2-D vision information is available to maintain formation. The methods for formation control rely either on estimating the range from 2-D vision information by using Extended Kalman Filters or directly regulating the size of the image subtended by a leader aircraft on the image plane. When the image size is not a reliable measurement, especially at large ranges, we consider the use of bearing-only information. In this case, observability with respect to the relative distance between vehicles is accomplished by the design of a time-dependent formation geometry. To improve the robustness of the estimation process with respect to unknown leader aircraft acceleration, we augment the EKF with an adaptive neural network. 2-D and 3-D simulation results are presented that illustrate the various approaches.**

I. Introduction

As demonstrated in recent events, unmanned aerial vehicles (UAVs) are becoming an important component of our military force structure. Looking forward, maintaining a formation while executing missions in the presence of terrain and obstacles is seen as an important challenge. It will also remain important to minimize communication between vehicles. In this paper, we focus on measurement, estimation and formation control guidance strategies [1]-[3].

Although imperfectly understood, flocking behavior of birds, schooling behavior of fish, and even studies of swarming insects have provided inspiration for concepts of coordinated multi-vehicle operation [4]. Existing work on coordinated group motion include a distributed behavioral approach to synthesizing the flocking motion of boids [5] (bird and fish-like objects). It was shown in [6] that coordinated multi-robot motion could be constructed by using a small basis set of behaviors. A control-theoretic approach to vision-based formation control is given in [7]. The control laws allow each follower vehicle in the formation to regulate range and relative orientation with respect to one leader vehicle, or range with respect to two leader vehicles, or range with respect to a leader vehicle while maintaining safe distance from obstacles. Switching between the control laws leads to changes in formation shape. Related work on formation control includes assignment of feasible formations [8] and moving into formation [9].

Most of the approaches for formation control assume that a leader vehicle state of motion is known at least partially to the follower (neighboring) vehicles [2][8]. The approach taken here is to observe these quantities through passive vision information. That is, a single camera is provided with a view of another aircraft, and that imagery is processed in real-time to determine other aircraft state information. We assume that the image is represented in terms of a noisy measurement of image center and size [15]. Range or depth information is not directly available.

We utilize the vision information from two different perspectives. In one approach, we construct an Extended Kalman filter (EKF) to estimate relative velocity and position [14], [15], which we utilize in the guidance policy. In the second approach, the guidance policy is based on directly regulating the vision (image-plane) measurements, for e.g., regulate the image position to be in the center of the image plane and image size to a specified size.

The image size measurement is not a viable measurement at large ranges, and in this case we rely on bearing information. This represents a "worst case" for vision-based formation control. By applying an EKF to the bearing measurement, estimates of the relative position and

This work was supported in part by AFOSR MURI #F49620-03-1-0401: Active Vision Control Systems for Complex Adversarial 3-D Environments.

E. N. Johnson is the Lockheed Martin Assistant Professor of Avionics Integration, School of Aerospace Engineering, Georgia Institute of Technology, Atlanta, GA 30332-0150 USA (phone: 404-385-2519; e-mail: Eric.Johnson@ae.gatech.edu).

A. J. Calise is Professor of Aerospace Engineering, Georgia Institute of Technology, Atlanta, GA 30332-0150 USA (e-mail: Anthony.Calise@ae.gatech.edu).

R. Sattigeri is a Graduate Research Assistant, School of Aerospace Engineering, Georgia Institute of Technology, Atlanta, GA 30332-0150 USA (e-mail: gte334x@mail.gatech.edu).

Y. Watanabe is a Graduate Research Assistant, School of Aerospace Engineering, Georgia Institute of Technology, Atlanta, GA 30332-0150 USA (e-mail: gtg341p@mail.gatech.edu).

V. Madyastha is a Graduate Research Assistant, School of Aerospace Engineering, Georgia Institute of Technology, Atlanta, GA 30332-0150 USA (e-mail: gt6405c@mail.gatech.edu).

velocity are obtained of each vehicle in the formation by every other vehicle. In general, regardless of the approach taken to processing vision-based data, the distance between one vehicle and any other vehicle is difficult to estimate. If we use poor range estimates to control a vehicle performing station-keeping with the target, a dangerous proximity may occur. It is well known that the accuracy of range estimation depends on camera translating motion, and the best translation for range estimation is a motion parallel to its image plane [13].

Another associated problem is the influence of the unknown target aircraft acceleration on the estimates provided by the EKF. The unknown acceleration acts as unmodeled disturbances on the estimation process, giving rise to biased or even diverging estimates. In this paper, we discuss a method to augment an EKF with a neural network (NN) based adaptive element that provides robustness to unknown and unmodeled dynamics. In a complementary approach, the nominal guidance policy associated with regulating the vision measurements is augmented with the output of an adaptive NN that compensates for the effect of target aircraft motion on the dynamics of these measurements.

Obstacle avoidance is a problem that, in general, cannot be completely separated from that of maintaining a formation, as obstacle avoidance considerations must take precedence. There are numerous approaches to static obstacle avoidance. A popular approach is the Artificial Potential Field Approach [10]. Other approaches include Motion Planning [11] and "Steer Towards Silhouette Edge" [12]. In this paper we describe and implement the latter approach, as in [17].

The organization of the paper is as follows. Section II summarizes the theory for vehicle state estimation, and states the problem formulation for formation control. Section III describes the guidance strategy for formation control. Section IV describes the approach to avoiding static obstacles. Section V describes an adaptive guidance approach based on directly regulating the image plane measurements. In Section VI we present and discuss simulation results for each approach. Section VII briefly describes our 6 DOF image-in-the-loop simulation capability.

II. Bearing-Only Target State Estimation

A. Filter design

Here, the EKF formulation described in [14] is utilized per other vehicle that requires state estimation. At most, this could include all vehicles in the formation estimating the state of all others. The four states used per filter have the dynamics

$$\frac{d}{dt}\begin{bmatrix} \dot{\beta} \\ \frac{\dot{r}}{r} \\ \beta \\ \frac{1}{r} \end{bmatrix} = \begin{bmatrix} -2\dot{\beta}\frac{\dot{r}}{r} + \frac{1}{r}\left(a_y \cos\beta - a_x \sin\beta\right) \\ \dot{\beta}^2 - \left(\frac{\dot{r}}{r}\right)^2 + \frac{1}{r}\left(a_y \sin\beta + a_x \cos\beta\right) \\ \dot{\beta} \\ -\frac{\dot{r}}{r}\frac{1}{r} \end{bmatrix}. \quad (1)$$

where β is the bearing to the other aircraft, r is the range, and a_x and a_y are the horizontal relative acceleration components in a Cartesian frame, i.e., the acceleration of the target minus the acceleration of the platform doing the estimation. These components are illustrated in figure 1, for aircraft i tracking aircraft j.

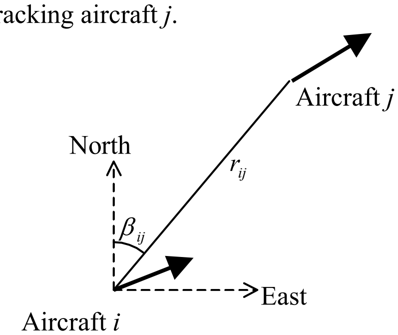

Fig. 1. Illustration of parameters for tracking of aircraft j by aircraft i.

Here it assumed that each vehicle knows its own heading though typical sensing methods. As a result, the relative bearing information provided by vision sensing another aircraft is immediately converted to a bearing to the other aircraft. The acceleration of the platform doing the estimation is considered known through measurement.

B. Optimization

Analysis of the contributing factors to the range estimate covariance indicates that a large magnitude of $\dot{\beta}$ gives more accurate range estimation. This also makes sense physically, as viewing the tracked vehicle from a different direction will provide information about position in an additional dimension. From this analysis, it is concluded that $\dot{\beta}$ should be maximized in order to obtain an accurate range estimate. At the same time, it is preferred that the relative bearing stay close to its prescribed desirable value. Also, it is important to limit the acceleration $\ddot{\beta}$. Therefore, an optimization problem that maximizes the predicted range estimation accuracy is formulated as

$$\min_{\ddot{\beta}} \int \{-\dot{\beta}^2 + \frac{K_1}{2}(\beta - \beta_d)^2 + \frac{K_2}{2}\ddot{\beta}^2\} dt$$

subject to the relative motion dynamics (1). The optimal solution can be derived by solving the Euler-Lagrange equations.

$$\beta = A_1 e^{a_1 t} + A_2 e^{a_2 t} + A_3 e^{a_3 t} + A_4 e^{a_4 t}$$

$$K_2 a_i^{\,4} + 2a_i^{\,2} + K_1 = 0$$

If we choose K_1 and K_2 which satisfy $K_1 K_2 = 1$, then β becomes simply [16]

$$\beta = A\cos\omega t + B\sin\omega t\,, \quad \omega = \sqrt{K_1}\ .$$

C. Adaptive Estimation

A method for augmenting a linear time invariant estimator with a NN based adaptive element was described in [20]. This approach has recently been extended to augment an EKF [21]. These approaches provide robustness to unknown and unmodeled dynamics in the process. A critical application of the adaptive EKF lies in the realm of tracking maneuvering targets, particularly in the bearings-only target-tracking problem. It is well known in the target-tracking literature that the accuracy of the resulting EKF estimates depends extensively on the target behavior. The universal approximation property of NNs has paved the way for NN-based identification and estimation schemes that may account for these unknown modeling errors/uncertainties in the process. The training signal for the NN is generated by the residuals produced by the EKF. The residuals are the difference between the image plane measurements and the EKF estimates.

III. Formation Guidance Strategy

Here, a leader takes the formation along the desired trajectory. This trajectory is unknown to the other, follower, aircraft. The follower aircraft each attempt to maintain a prescribed time-dependent relative position to the leader.

The relative position is time-dependent to ensure observability of range to the leader. Collision hazards between following aircraft are prevented by careful selection of these chosen relative positions; mitigating the need for robust estimation of other aircraft state for anything but the leader. Here, the commanded distance is set to a constant, and the angle is varied periodically by a small amount.

Each follower generates a lateral and longitudinal acceleration command to bring it to the prescribed relative position with a second order response, utilizing its position and velocity estimates for the leader aircraft. An aircraft performance model then limits this acceleration command.

However, all aircraft will depart from these strategies as necessary to avoid obstacles. This is the subject of the next section.

IV. Static Obstacle Avoidance

The controller design strategy for static obstacle avoidance is based on a reactive "steer towards silhouette edge" approach [12]. The idea is to project the shape of nearby obstacles onto the local, velocity-fixed frame of the vehicle. If this projected shape, adjusted (enlarged) to allow for the size of the vehicle and uncertainty, surrounds the origin of the velocity frame, then some portion of the obstacle is dead ahead (see figure 2). The vehicle must steer away to avoid a collision, and the most efficient direction to turn is toward the portion of the projected shape that is closest to the origin.

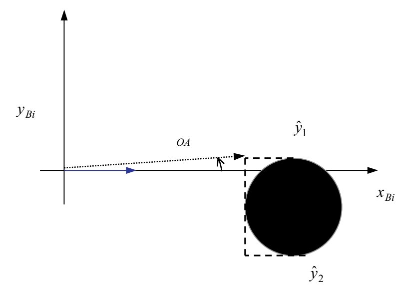

Fig. 2. Illustration of obstacle avoidance approach described here. Lateral acceleration required to miss target is applied once it exceeds a threshold value.

To illustrate the concept, it is assumed that the obstacles are contained within bounding spheres (circles in 2 dimensions), and that the centers X_O, Y_O and radii r_O of the obstacles are known. The goal of this strategy is to keep an imaginary line L_O of length D_O, originating at the vehicle current position and extending in the direction of the velocity vector, from intersecting with any obstacle boundary [5]. The length of this line is typically based upon the vehicle's speed and maneuverability. An obstacle further away than this length D_O is not an immediate threat.

Corrective steering action to avoid an obstacle involves a speed and heading change command. The heading change command $\Delta\psi_{OA}$ is towards the closest projected edge of the obstacle as shown in figure 2. No speed change is used. The corresponding lateral acceleration command can replace the formation flight command when obstacle avoidance is required. When the hazard has passed, the vehicle then returns to the formation.

V. Subtended-Angle Guidance Approach

The paper by Betser et. al. [15] in this session shows how additional information from the imaging camera can be used to make the range estimation process more robust to the leader (target) acceleration. The additional information is the angle subtended by the leader aircraft on the image plane, referred to as the subtended angle α. However, leader acceleration can still cause problems by giving rise to biased estimates of range.

An alternative approach would be to directly regulate the subtended angle to a desired value instead of the range. The subtended angle α is given by

$$\alpha = 2\tan^{-1}\left(\frac{\delta}{2r}\right)$$

where δ is a leader aircraft representative size (e.g., wing-span). The subtended angle dynamics can be written as

$$\dot{\alpha} = -\frac{2}{\delta}(1-\cos\alpha)\dot{r}$$

by assuming $\dot{\delta} = 0$. The guidance strategy involves inverting the $\dot{\alpha}$ equation to get a desired velocity vector for the follower aircraft. Noting that the range-rate term $\dot{r}$ involves the leader aircraft velocity along the LOS, we can augment the nominal inverting solution with the output of an adaptive NN to compensate for this leader velocity. This approach is identical to that shown in Ref. [17] where range is the regulated variable. The approach requires that noisy visual information be directly input to the adaptive NN, along with velocity and heading information. The adaptive guidance approach is robust to vehicle dynamics that are neglected in the process of treating velocity as control, and to parametric uncertainties that arise from not knowing the exact leader aircraft size δ.

VI. Simulation Results

Figures 3 and 4 show results obtained with the bearings-only, non-adaptive target state estimation approach. We consider a team of 3 aircraft flying in formation in a 2 dimensional environment in the presence of obstacles. Aircraft #2 is the leader. It sets the trajectory for the formation by commanding a sequence of heading changes while maintaining a constant speed. Each follower aircraft regulates to a time-dependent relative position to the leader. In addition, the 3 aircraft are also commanded to avoid obstacles.

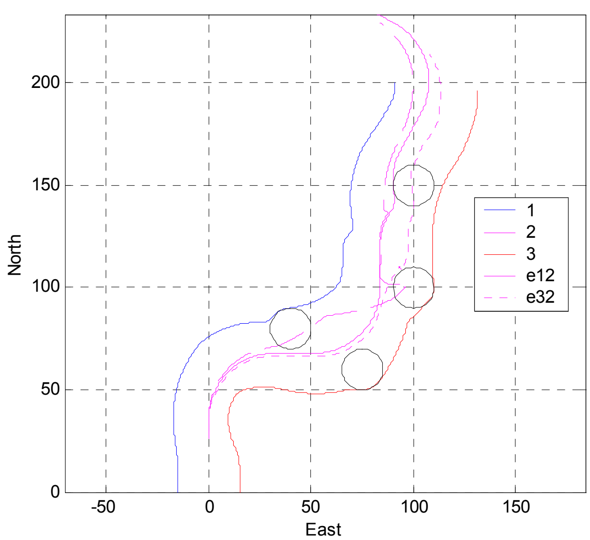

Fig. 3. Ground track of a typical result. The formation starts at the bottom, and proceeds to the top. Aircraft #2 (center) is the leader. The estimated positions for the leader are also plotted for both followers. Both followers and the leader are occasionally required to maneuver to avoid one of the four fixed obstacles. Without utilizing a time-dependent formation shape, range tends to be under-predicted.

The ground track for a typical simulation result is illustrated in figure 3. The leader performs a series of left and right turns, although during one of the turns it must avoid an obstacle instead. The two followers also occasionally must avoid one of the four obstacles. The position estimate for the leader is also shown for each of the two followers. Here, the relative commanded position is held constant, and estimation performance suffers.

A slight periodic time dependency is added for the result in figure 4. The changes in commanded relative position, yields acceptable estimation performance.

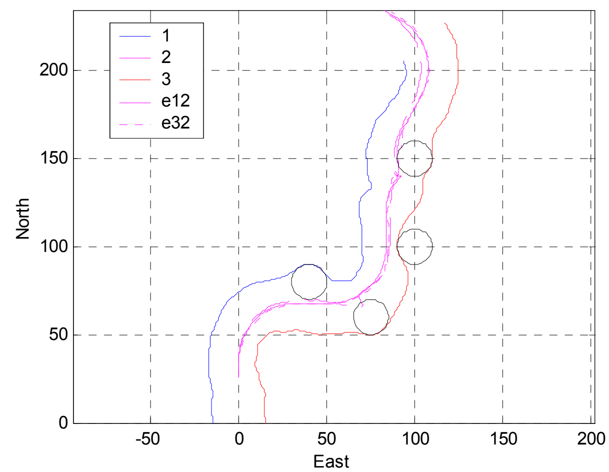

Fig. 4. The formation starts at the bottom, and proceeds to the top. Aircraft #2 (center) is the leader. The estimated positions for the leader are improved by slight periods changes in formation shape.

Figure 5 shows tracking results with a highly maneuvering leader aircraft. Only 1 follower aircraft is included in this simulation. The leader aircraft commands a sinusoidal heading maneuver at constant speed. The upper plot shows the trajectory of the leader, and the follower and an estimate of the leader trajectory by the follower. The bottom plot shows the true range, estimated range by the Follower and the commanded range. The reason for the poor estimates is that the model for the leader acceleration used in the estimation process is highly inaccurate. Figure 6 show results for the same leader aircraft maneuver obtained by augmenting the EKF with an adaptive NN, where the true and estimated ranges correspond very well, indicating that the NN is able to reconstruct target acceleration.

Figures 7 and 8 show results for regulating the subtended angle to commanded value α_{com} for the same sinusoidal leader aircraft maneuver. The command value α_{com} corresponds to a command range equal to 2 wing-span lengths. Figure 7 shows the result with the nominal guidance policy that does not account for leader aircraft motion.

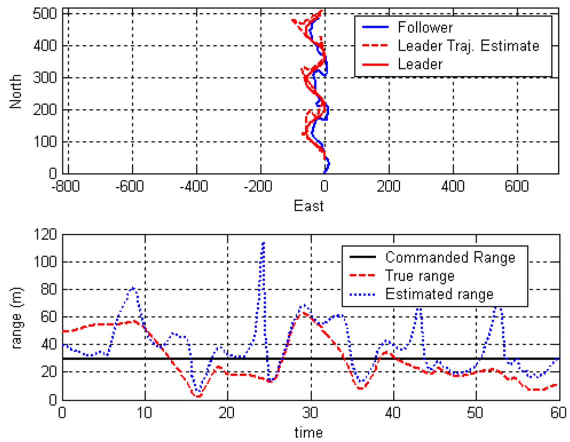

Fig. 5. Range Estimation for a sinusoidally maneuvering leader with *non-adaptive* bearings-only approach. The estimated range varies significantly from the true range because the Leader acceleration is not accurately modeled in the estimation process.

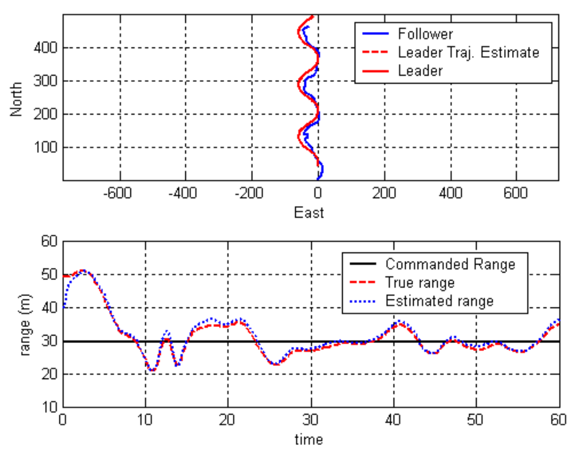

Fig. 6. Range Estimation for a sinusoidally maneuvering leader with *adaptive* bearings-only approach. The range estimation is excellent compared to the non-adaptive bearings only approach, the NN is able to reconstruct target acceleration.

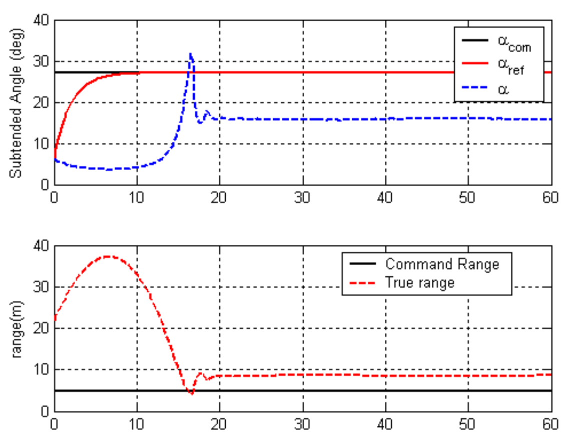

Fig. 7. Subtended Angle regulation with nominal guidance policy. The steady-state tracking error is due to neglecting leader aircraft motion.

An estimate for the leader aircraft size equal to 1.2 times the true size is used when inverting the α dynamics. The effect of neglecting the leader aircraft motion shows up as steady-state error in the subtended angle regulation. In the above plot, α_{ref} refers to a reference α obtained by filtering α_{com} through a first-order command filter. Figure 8 shows the subtended angle regulation obtained by augmenting the nominal guidance policy with the output of an adaptive NN. The reference command α_{ref} does not coincide with command α_{com} after the initial transient because the command filter is *hedged* [18] to protect the adaptive process from control saturation.

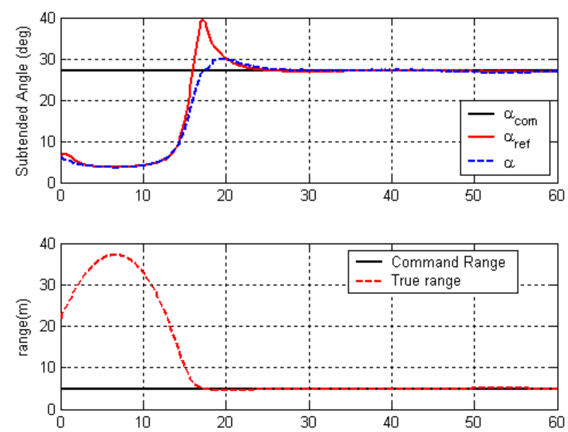

Fig. 8. Subtended Angle regulation with adaptive guidance policy.

VII. 6 DOF Image-in-the-Loop Simulation

The relative position and velocity estimator discussed in the previous section is extended to 3-dimensions and applied to a formation flight of two airplanes. Estimation results of 6 DOF image-in-the-loop simulations are shown in this section. Figure 9 shows a display of the 6 DOF airplane simulator. It includes two airplanes, configured as leader and follower. The follower aircraft has a camera and its image is also simulated. The synthetic images are processed and providing the same type of output we expect in an actual flight [19].

The image processor provides a position and size (wingspan) of the leader in camera images. From those measurements, the filter is designed to estimate relative position and velocity between the two aircraft. In order to avoid singularity occasions, a filter state and a measurement vector are chosen as follows.

$$\boldsymbol{x} = \begin{bmatrix} \boldsymbol{u}^T & \dot{\boldsymbol{u}}^T & \frac{1}{r} & \frac{\dot{r}}{r} & b \end{bmatrix}^T, \ \boldsymbol{z} = \begin{bmatrix} \boldsymbol{u} \\ \alpha \end{bmatrix}$$

where $\boldsymbol{u}$ is a unit vector pointing to the leader, r is the distance between the two aircraft, b is the wingspan of the leader, and α is the subtended angle.

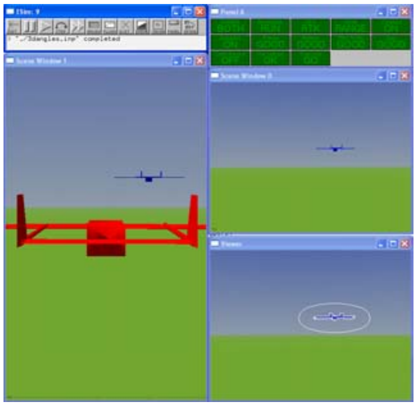

Fig. 9. 6 DOF image-in-the-loop airplane simulator. Two airplanes (blue=leader, red=follower) are shown. Right top window shows a simulated camera image and the bottom one displays outputs of the image processor.

We consider the case in which the follower aircraft is guided to change its relative position to the leader obeying a box-shaped command, while the leader flies straight with a constant speed. Figure 10 shows estimation results of relative position. The position x is approximately the range between the two aircraft.

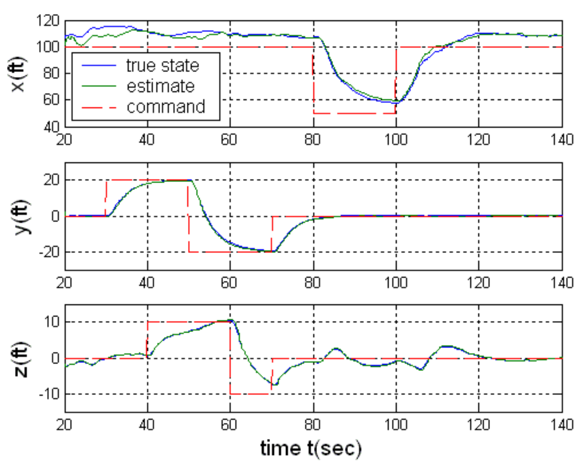

Fig. 10. Relative position estimation. The Follower is guided by a relative position command (dashed red line).

VIII. Conclusions

In this paper, several approaches for vision-based formation control of multiple aircraft are implemented. No communication is required between vehicles, and simple passive vision processing is assumed, sufficient only to provide noisy bearing and image size measurements. Effects of unmodeled leader aircraft acceleration on the estimation and guidance processes are shown, and two adaptive methods to compensate for the same are discussed and demonstrated in simulation.

Acknowledgment

The authors wish to acknowledge the contributions, discussions, and advice from Allen Tannenbaum, Patricio Vela, Amir Betser, and Johnny Evers.

References

[1] A. Proud, M. Pachter, and J. J. D'Azzo, "Close Formation Control," *AIAA Guidance, Navigation and Control Conference*, Portland, OR, August 1999.

[2] C. J. Schumacher and R. Kumar, "Adaptive Control of UAVs in Close-Coupled Formation Flight," American Control Conference, Chicago, IL, June 2000, pp. 849-853.

[3] M. R. Anderson and A. C. Robbins, "Formation Flight as a Cooperative Game," *AIAA Guidance, Navigation and Control Conference*, Reston, VA, August 1998.

[4] E. Bonabeau, M. Dorigo, and G. Theraulaz, *Swarm intelligence: from natural to artificial systems*, Oxford University Press, 1999.

[5] C. W. Reynolds, "Flocks, Herds and Schools: a Distributed Behavioral Model," *Computer Graphics*, 21(4): 71-87,1987.

[6] M. Mataric, "Interaction and Intelligent Behavior," PhD thesis, MIT, EECS, 1994.

[7] A. V. Das, R. Fierro, V. Kumar, J. P. Ostrowski, J. Spletzer, and C. J. Taylor, "A Vision-based Formation Control Framework," *IEEE Trans. on Robotics and Automation*, Vol. 18, No. 5, October 2002, pp 813-825.

[8] P. Tabuada, G. Pappas, and P. Lima, "Feasible Formations of Multi-Agent Systems," *American Control Conference*, Arlington, VA, June 2001, pp. 56-61.

[9] H. Yamaguchi and T. Arai, "Distributed and Autonomous control method for generating shape of multiple mobile robot group," *Proc. IEEE International Conf. on Intelligent Robots and Systems*, Vol 2., 1994, pp. 800-807.

[10] O. Khatib, "Real-Time Obstacle Avoidance for Manipulators and Mobile Robots," *International Journal of Robotics Research*, 1986.

[11] E. Frazzoli and M. Dahleh, "Real-time Motion Planning for Agile Autonomous Vehicles," *American Control Conference*, June 2001, pp. 43-49.

[12] C. Reynolds, "Not Bumping Into Things," Notes on "obstacle avoidance" for the course on Physically Based Modeling at SIGGRAPH 88. Available: http://www.red3d.com/cwr/nobump/nobump.html

[13] L. Metthies and T. Kanade, "Kalman Filter-based Algorithms for Estimating Depth from Image Sequences," *International Journal of Computer Vision*, 3:209-236, 1989.

[14] V. J. Aidala and S. E. Hammel, "Utilizing of modified polar coordinates for bearings-only tracking," *IEEE Trans. Automatic Control*, 28:283-294, 1983.

[15] A. Betser, P. Vela, and A. Tannenbaum, "Automatic Tracking of Flying Vehicles Using Geodesic snakes and Kalman filtering," Submitted to: *IEEE Conference on Decision and Control*, 2004.

[16] Y. Watanabe, E.N. Johnson, and A.J. Calise, "Optimal 3-D Guidance from a 2-D Vision Sensor," *AIAA Guidance, Navigation, and Control Conference,* Providence, RI, August 2004.

[17] R. Sattigeri,, A. J. Calise, and J. H. Evers, "An adaptive vision-based approach to decentralized formation control," *AIAA Guidance, Navigation, and Control Conference,* Providence, RI, August 2004.

[18] Johnson, E., and Calise, A.J., "Neural Network Adaptive Control of Systems with Input Saturation," *American Control Conference*, Arlington, VA, June 2001, pp. 3527-3532.

[19] J. Ha, C. Alvino, G. Prior, M. Niethammer, E. N. Johnson and A. Tannenbaum, "Active Contours and Optical Flow for Automatic Tracking of Flying Vehicles," *American Control Conference*, 2004.

[20] N. Hovakimyan, A. Calise, V. Madyastha, "An Augmenting Adaptive Observer Design Methodology for Nonlinear Processes," *Proc. IEEE Conf. On Decision and Control,* vol. 4, Dec. 2002, pp. 4700-4705.

[21] V. Madyastha, and A.J. Calise, "An Adaptive Filtering Approach to Target Tracking," Submitted to *American Control Conference*, 2005.